



Dependence of North–South Difference in the Slope of Joy’s Law on the Amplitude of Solar Cycle

J. Javaraiah¹

Received: 4 November 2022 / Accepted: 19 August 2023 / Published online: 13 September 2023
© The Author(s), under exclusive licence to Springer Nature B.V. 2023

Abstract

Study of the tilt angles of solar bipolar magnetic regions is important because the tilt angles have an important role in the solar dynamo. We analyzed the data on tilt angles of sunspot groups measured at the Mt. Wilson Observatory (MWOB) during the period 1917–1986 and Kodaikanal Observatory (KOB) during the period 1906–1986. We binned the daily tilt-angle data during each of the Solar Cycles 15–21 into different 5°-latitude intervals and calculated the mean value of the tilt angles in each latitude interval and the corresponding standard error. We fitted these binned data to Joy’s law (increase of the tilt angle with latitude), i.e. the linear relationship between tilt angle and latitude of an active region. The linear least-square fit calculations were carried out by taking into account the uncertainties in both the abscissa (latitude) and ordinate (mean tilt angle). The calculations were carried out by using both the tilt-angle and area-weighted tilt-angle data in the whole sphere, northern hemisphere, and southern hemisphere during the whole period and during each individual solar cycle. We find a significant difference (north–south asymmetry) between the slopes of Joy’s laws recovered from northern and southern hemispheres’ whole-period MWOB data of area-weighted tilt angles. Only the slope obtained from the southern hemisphere’s MWOB data of a solar cycle is found to be reasonably well anticorrelated to the amplitude of the solar cycle. In the case of area-weighted tilt-angle data, a good correlation is found between the north–south asymmetry in the slope of a solar cycle and the amplitude of the solar cycle. The corresponding best-fit linear equations are found to be statistically significant.

Keywords Sun: dynamo · Sun: solar activity · Sun: sunspots

1. Introduction

The tilt angles of bipolar magnetic regions are one of the important ingredients for solar-dynamo models (Bhowmik and Nandy, 2018, and references therein). Tilt angles have a significant role in the generation of polar magnetic fields and the reverse of polarity of polar fields in a 22-year solar magnetic cycle. The tilt angles and Joy’s law (increase of tilt

Formerly working at Indian Institute of Astrophysics, Bengaluru-560 034, India.

✉ J. Javaraiah
jajj55@yahoo.co.in; jdotjavaraiah@gmail.com; jj@iiap.res.in

¹ Bikasipura, Bengaluru, 560 111, India

angle with latitude) depend on several properties of solar magnetic-active regions (sunspot groups), e.g. latitude, area, formation and evolution, rotation, and meridional motions, and also on solar-cycle phase (Howard, 1991; Sivaraman, Gupta, and Howard, 1999; Muneer and Sing, 2002; Zharkova and Zharkov, 2008). Dasi-Espuig et al. (2010) analyzed Mt. Wilson Observatory (1917–1986) and Kodaikanal Observatory (1906–1986) sunspot-group tilt-angle data and found the existence of a reasonably good anticorrelation between the ratio of mean tilt angle [$\langle \gamma \rangle$] over a solar cycle to mean absolute latitude [$\langle |\lambda| \rangle$] over the same solar cycle and the strength/amplitude of the solar cycle (note that $\langle \cdot \rangle$ implies the mean over a time interval, i.e. here over a solar cycle). Some authors confirmed this result and some others criticized it for various reasons (Jiao, Jiang, and Wang, 2021). There exists a considerable north–south difference/asymmetry in strengths/amplitudes of many solar cycles (e.g. Carbonell, Oliver, and Ballester, 1993; Verma, 1993; Norton and Gallagher, 2010; McIntosh et al., 2013; Javaraiah, 2019; Ravindra, Chowdhury, and Javaraiah, 2021). North–south asymmetry also exists in the rotational and the meridional motions of solar plasma, magnetic field, and tracers such as sunspot groups (Hathaway and Wilson, 1990; Javaraiah and Gokhale, 1997; Haber et al., 2002; Javaraiah, 2003; Gigolashvili et al., 2005; Javaraiah and Ulrich, 2006; Xie, Shi, and Qu, 2018; Lekshmi, Nandy, and Antia, 2018; Wan and Gao, 2022). It is believed that the action of Coriolis forces on rising magnetic-flux tubes is responsible for the tilts of bipolar active regions and Joy’s law (see D’Silva and Choudhuri, 1993; Fisher, Fan, and Howard, 1995; Bhowmik and Nandy, 2018; Jiao, Jiang, and Wang, 2021). Since there exists north–south asymmetry in the solar rotation, there could be a difference in the action of Coriolis forces on the rising magnetic-flux tubes in the northern and southern hemispheres. Therefore, north–south asymmetry may exist in the slope of Joy’s law and it also may depend on the amplitude of the solar cycle. McClintock and Norton (2013) analyzed the Mt. Wilson sunspot-group data (1917–1986) and found the aforementioned result (anticorrelation between $\langle \gamma \rangle / \langle |\lambda| \rangle$ and strength of cycle) from the southern hemisphere’s data, but not from the northern hemisphere’s data. Dasi-Espuig et al. (2010) and McClintock and Norton (2013) used $\langle \gamma \rangle / \langle |\lambda| \rangle$ to remove the effect of latitudinal dependence of mean tilt angle in the relation between the mean tilt angle and the strength of the solar cycle. However, the anticorrelation between $\langle \gamma \rangle$ alone and the strength of a solar cycle is statistically insignificant. Therefore, one may doubt that the existence of a good correlation between $\langle |\lambda| \rangle$ and the strength/amplitude of a solar cycle has a significant influence on the aforementioned result. That is, the significant anticorrelation between $\langle \gamma \rangle / \langle |\lambda| \rangle$ and the strength/amplitude of a solar cycle might be largely an artifact of the good correlation between the denominator [$\langle |\lambda| \rangle$] of $\langle \gamma \rangle / \langle |\lambda| \rangle$ and the strength/amplitude of the solar cycle. It is difficult to differentiate the coefficients of Joy’s law (namely the slope of the linear relation between tilt angle and latitude) of different solar cycles due to large uncertainties in the derived coefficients (Dasi-Espuig et al., 2010). Hence, Dasi-Espuig et al. (2010) and McClintock and Norton (2013) did not calculate the correlation between the slope of Joy’s law and the amplitude/strength of a solar cycle. In the present analysis, by using the same aforementioned data of tilt angles of the sunspot groups measured at the Mt. Wilson Observatory (MWOB) during the period 1917–1986 and the Kodaikanal Observatory (KOB) during the period 1906–1986, we study the dependence of the slope of Joy’s law (coefficient of Joy’s law) on the amplitude of the solar cycle by determining it from the whole-sphere data and northern and southern hemispheres’ data. We obtain the relationship between the slope (and its north–south asymmetry) and the amplitude of the solar cycle by determining the linear least-square fits to the data of these parameters taking into account the uncertainties in all these parameters.

In the next section we describe the data and analysis. In Section 3 we describe the results, and in Section 4 we present the conclusions and briefly discuss them.

2. Data Analysis

Here, we use the daily data: heliographic latitude (area weighted) $[\lambda]$, area $[A]$, tilt angle $[\gamma]$, etc. of sunspot groups measured at the Mt. Wilson Observatory (MWOB) during the period 1917–1986, and the Kodaikanal Observatory (KOB) during the period 1906–1986. These data are available at the website www.ngdc.noaa.gov/stp/solar/sunspotregionsdata.html. We had used these data in an earlier analysis of angular velocities of sunspot groups (Javaraiah, Bertello, and Ulrich, 2005). In both the northern and southern hemispheres a positive tilt angle implies that the leading spot is closer to the Equator than the following spot. We use the amplitudes 175.7 ± 11.8 , 130.2 ± 10.2 , 198.6 ± 12.6 , 218.7 ± 10.3 , 285.0 ± 11.3 , 156.6 ± 8.4 , and 232.9 ± 10.2 (values of R_M , the maximum 13-month smoothed monthly mean values of Version-2 of the international sunspot number, SN) of Solar Cycles 15, 16, 17, 18, 19, 20, and 21, respectively (taken from Pesnell, 2018). Here, the data reduction and analysis are similar to that in Dasi-Espuig et al. (2010) and McClintock and Norton (2013). We excluded the data corresponding to zero values of the tilt angles, and also those corresponding to the difference between the tilt angles of a sunspot group observed in two consecutive days being $\geq 16^\circ \text{ day}^{-1}$. We binned the daily tilt-angle data during each of the Solar Cycles 15–21 into seven different 5° -latitude (absolute) intervals $0-5^\circ$, $5-10^\circ$, $10-15^\circ$, $15-20^\circ$, $20-25^\circ$, $25-30^\circ$, and $30-35^\circ$. We calculated the mean value $[\bar{\gamma}]$ of the tilt angles, and the corresponding standard error in each latitude bin. We fitted these data to Joy’s law in the form:

$$\bar{\gamma} = m|\lambda| + c, \quad (1)$$

where λ is the mid-value of a latitude bin (in the case of area-weighted tilt angles, $\bar{\gamma}_{aw}$ is used instead of $\bar{\gamma}$). Here, the slope m is referred to as the coefficient of Joy’s law. The calculations of linear least-square fits were carried out by taking into account the uncertainties in both the abscissa $[\lambda]$ and the ordinate $[\bar{\gamma}]$, namely the standard error in the case of $\bar{\gamma}$ and the value 2.5° , i.e. half of the range of a latitude interval, in the case of $|\lambda|$. The calculations were carried out by using the tilt-angle data and also the area-weighted tilt-angle data of the whole sphere, and separately for northern and southern hemisphere tilt-angle data. The area-weighted mean tilt angle $[\sum(\gamma_i \times A_i) / \sum A_i = X/Y]$ where X is the mean of $(\gamma_i \times A_i)$, Y is the mean of A_i , $i = 1, \dots, n$, and n is the number of data points in a given latitude bin. If $\Delta(X)$ and $\Delta(Y)$ are the uncertainties in X and Y , respectively, then the uncertainty in the ratio X/Y will be approximately equal to $(Y \times \Delta(X) - X \times \Delta(Y))/Y^2$ (see also Javaraiah and Gokhale, 1997). Note that here $\Delta(X)$ and $\Delta(Y)$ represent the standard errors of X and Y , respectively. The coefficients of Joy’s law over the whole sphere and in northern and southern hemispheres were determined from the combined data of all cycles (15–21), and from the data of each individual cycle. The MWOB data of Solar Cycle 15 are incomplete (note that the beginning of this solar cycle was 1913). In the case of this solar cycle, the number of data points is found to be very few in the $30-35^\circ$ latitude bins of the northern hemisphere (zero in both MWOB and KOB data) and the southern hemisphere (6 and 2 in MWOB and KOB data, respectively). Hence, the data in this latitude bin are not considered in the linear least-square fits of this solar cycle’s data in all three cases: whole sphere, northern hemisphere, and southern hemisphere. We determined the correlation between the slope m and amplitude R_M during Solar Cycles 15–21. We also determined the corresponding linear regression. The separate northern and southern hemispheres’ sunspot-number data are not available for Solar Cycles 15–21. Hence, we compared the northern and southern hemispheres’ values of the slope of Joy’s law and the corresponding north–south asymmetry, with the amplitude R_M (maximum total sunspot number) of the solar cycle. All the linear

Table 1 Values of mean tilt angle [$\bar{\gamma}$, in deg.] and of mean area-weighted tilt angle [$\bar{\gamma}_{aw}$, in deg.] of sunspot groups in absolute latitude intervals $0-5^\circ$, $5-10^\circ$, $10-15^\circ$, $15-20^\circ$, $20-25^\circ$, $25-30^\circ$, and $30-35^\circ$ ($|\lambda|$ represents the mid-value of an absolute latitude interval) determined from the whole-sphere data, and separately from the northern and southern hemispheres' data, during the entire period. n represents the number of data points in each latitude interval. The uncertainties in $\bar{\gamma}$ and $\bar{\gamma}_{aw}$ are the corresponding standard errors.

$ \lambda $	Whole sphere			Northern hemisphere			Southern hemisphere		
	$\bar{\gamma}$	$\bar{\gamma}_{aw}$	n	$\bar{\gamma}$	$\bar{\gamma}_{aw}$	n	$\bar{\gamma}$	$\bar{\gamma}_{aw}$	n
Derived from Mt. Wilson data									
2.5	1.44 ± 0.76	3.32 ± 0.82	1670	0.79 ± 1.08	4.34 ± 1.34	820	2.06 ± 1.07	2.41 ± 0.98	850
7.5	2.43 ± 0.39	3.28 ± 0.43	5914	3.18 ± 0.56	3.78 ± 0.60	2845	1.73 ± 0.54	2.80 ± 0.62	3069
12.5	4.39 ± 0.34	5.08 ± 0.35	7719	4.40 ± 0.46	5.21 ± 0.48	4108	4.37 ± 0.50	4.93 ± 0.51	3611
17.5	4.84 ± 0.38	5.01 ± 0.42	6461	5.55 ± 0.53	5.75 ± 0.61	3310	4.10 ± 0.54	4.18 ± 0.58	3151
22.5	5.45 ± 0.48	6.31 ± 0.51	3881	6.11 ± 0.64	7.69 ± 0.64	2190	4.60 ± 0.73	4.55 ± 0.81	1691
27.5	6.56 ± 0.76	7.65 ± 0.80	1764	7.61 ± 1.02	9.58 ± 1.04	1051	5.02 ± 1.14	4.36 ± 1.23	713
32.5	6.72 ± 1.41	7.46 ± 1.57	544	7.03 ± 1.81	8.68 ± 1.98	318	6.28 ± 2.25	5.38 ± 2.57	226
Derived from Kodaikanal data									
2.5	2.19 ± 0.74	3.71 ± 0.91	1583	1.95 ± 1.01	4.84 ± 1.36	842	2.47 ± 1.09	2.23 ± 1.14	741
7.5	2.94 ± 0.40	3.81 ± 0.44	5732	3.65 ± 0.57	5.41 ± 0.62	2936	2.20 ± 0.56	1.90 ± 0.60	2796
12.5	4.56 ± 0.33	6.02 ± 0.36	7857	5.38 ± 0.45	6.25 ± 0.49	4111	3.67 ± 0.48	5.72 ± 0.53	3746
17.5	4.74 ± 0.39	4.88 ± 0.41	6480	5.31 ± 0.53	5.67 ± 0.57	3226	4.18 ± 0.57	4.01 ± 0.60	3254
22.5	5.31 ± 0.48	5.40 ± 0.55	4180	6.38 ± 0.62	6.29 ± 0.69	2418	3.85 ± 0.76	4.04 ± 0.92	1762
27.5	7.38 ± 0.73	9.37 ± 0.87	1866	7.12 ± 0.99	10.20 ± 1.30	1010	7.69 ± 1.09	8.36 ± 1.09	856
32.5	4.56 ± 1.38	6.91 ± 1.82	618	6.68 ± 1.70	8.71 ± 2.46	346	1.85 ± 2.28	4.28 ± 2.65	272

regression analyses presented in this article were carried out by using the Interactive Digital Library (IDL) software FITEXY.PRO, which is downloaded from the website idlastro.gsfc.nasa.gov/ftp/pro/math/. This software is very useful because the uncertainties of both the abscissa and ordinate will be accounted for in the calculations of linear least-square fitting.

3. Results

3.1. Recovering Joy's Law from the Combined Data of All Solar Cycles

In Table 1 we list the values of the mean tilt angle [$\bar{\gamma}$] and of the mean area-weighted tilt angle [$\bar{\gamma}_{aw}$] of sunspot groups in each absolute latitude intervals $0-5^\circ$, $5-10^\circ$, $10-15^\circ$, $15-20^\circ$, $20-25^\circ$, $25-30^\circ$, and $30-35^\circ$ ($|\lambda|$ represents the mid-value of an absolute latitude interval) separately determined from the data of sunspot groups in the northern and southern hemispheres and from the combined data (whole sphere data) during all solar cycles (15–21), i.e. data of sunspot groups measured at MWOB during the period 1917–1986 and at KOB during the period 1906–1986. The uncertainties in $\bar{\gamma}$ and $\bar{\gamma}_{aw}$ are the corresponding standard errors and n represents the number of data points in a latitude interval. As we can see in this table, the values of both $\bar{\gamma}$ and $\bar{\gamma}_{aw}$ are reasonably accurate (the ratio of mean value to standard error is large) except, particularly in the case of KOB data, at $|\lambda| = 32.5^\circ$ (i.e. in the $30-35^\circ$ latitude interval) of the southern hemisphere. Figure 1 shows the Joy's law derived from the data given in Table 1 for the whole sphere and Figures 2 and 3

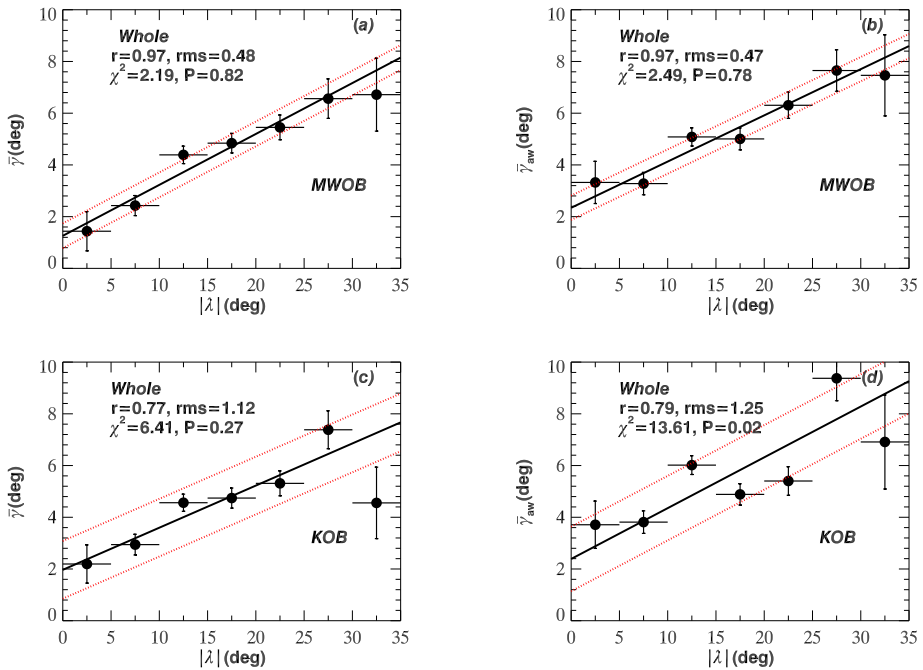


Figure 1 Mean tilt angle $[\bar{\gamma}]$ and mean area-weighted tilt angle $[\bar{\gamma}_{aw}]$ versus middle-value of the corresponding 5° latitude bin, determined from Mt. Wilson Observatory (MWOB) and Kodaikanal Observatory (KOB) whole-sphere sunspot-group data. The *continuous line* represents the corresponding linear least-square best fit and the *dotted line (red)* represents the one-rms level. The values of the correlation coefficient $[r]$, rms, and χ^2 and the corresponding probability $[P]$ are also given.

are the same as Figure 1, but the Joy’s laws are derived from the northern and southern hemispheres’ data, respectively. In all these figures, the values of the correlation coefficient $[r]$, rms (root-mean-square deviation), χ^2 , and the corresponding probability $[P]$ are given, and in Table 2 the details on the best-fit linear equations are given. As we can see in these figures and in Table 2, all the linear relations (Joy’s laws) derived from particularly MWOB data are good, i.e. the values of r are sufficiently high, the values of χ^2 are significantly lower, and the ratios of the slopes to the corresponding standard deviations are substantially higher. Overall, the relations derived from KOB data are relatively less reliable, in particular, the relations correspond to both the tilt-angle and the area-weighted tilt-angle data of the southern hemisphere are statistically insignificant (see Figures 3c and d).

As we can see in Table 2, there exist some differences in the values of the slopes of the linear equations obtained from MWOB and KOB data. These differences are statistically significant in the case of area-weighted tilt-angle data of both the northern and southern hemispheres. The values of the slopes determined from the MWOB and KOB whole-sphere tilt-angle data well match within their uncertainties limits with the value 0.2 that was obtained by Norton and Gilman (2005) by using tilt angles of 650 active regions observed in *Michelson Doppler Imager* data during the period 1996–2004. Both MWOB and KOB whole-sphere values of the slopes (determined from both the tilt-angle and area-weighted tilt-angle data) are slightly lower than the corresponding values 0.26 ± 0.05 and 0.28 ± 0.06 that were obtained from the area-weighted tilt-angle data by Dasi-Espuig et al. (2010) by forcing the linear fit through the origin. The values of northern and southern hemispheres’

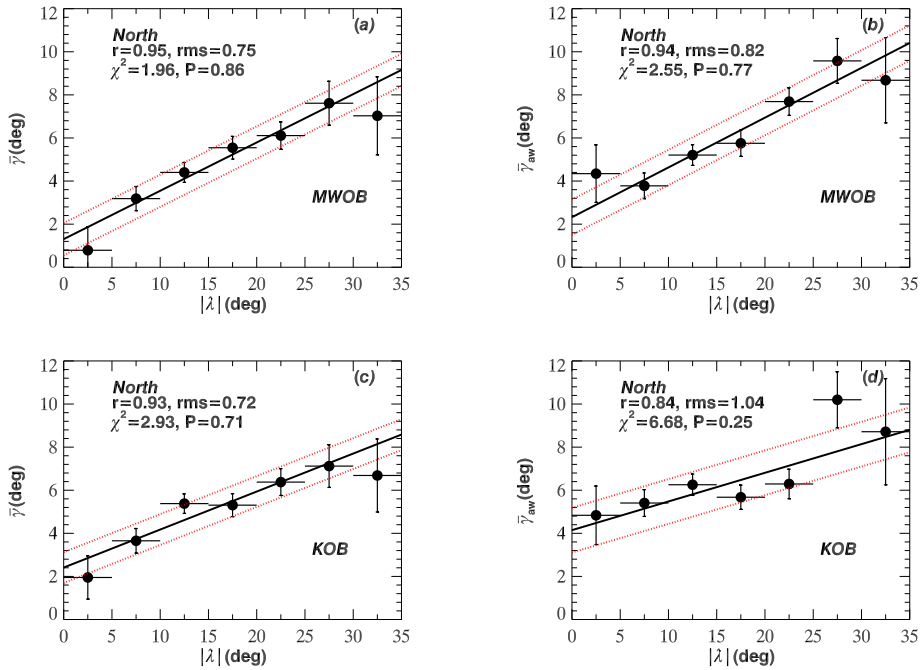


Figure 2 Mean tilt angle $[\bar{\gamma}]$ and mean area-weighted tilt angle $[\bar{\gamma}_{aw}]$ versus middle-value of the corresponding 5° latitude bin, determined from Mt. Wilson Observatory (MWOB) and Kodaikanal Observatory (KOB) northern hemisphere sunspot-group data. The *continuous line* represents the corresponding linear least-square best fit and the *dotted line (red)* represents the one-rms level. The values of the correlation coefficient $[r]$, rms, and χ^2 and the corresponding probability $[P]$ are also given.

slopes determined from MWOB area-weighted tilt-angle data reasonably match the corresponding values 0.26 and 0.13 determined from the same data by McClintock and Norton (2013). In the case of MWOB area-weighted tilt-angle data, the slope of the northern hemisphere is significantly (more than 95% confidence level) larger ($\approx 130\%$) than that of the southern hemisphere. In the case of KOB data, the slope corresponding to the area-weighted tilt-angle data of the southern hemisphere looks to be larger than that of the northern hemisphere, but as already mentioned above, the relations obtained from the KOB southern hemisphere’s data are unreliable. Hence, in this case it is not possible to draw any conclusion on the north–south difference in the slope.

3.2. Recovering Joy’s Law from the Data of Individual Solar Cycles

In this section we find no significant results from KOB data. Here, we present only the results derived from MWOB data. We do not know the exact reason for the discrepancies in the results derived from KOB and MOB data, but during some solar cycles the KOB data seem to be more inconsistent due to a large number of missing observations (Ravindra, Chowdhury, and Javaraiah, 2021).

In Table 3 we list the values of the intercept $[c]$, slope $[m]$, and the corresponding standard deviation $[\sigma]$ of the best-fit linear relationships derived from mean values of tilt angles and area-weighted tilt angles of sunspot groups in different 5° absolute-latitude intervals of the whole sphere during each solar cycle. The values of the correlation coefficient r , χ^2 ,

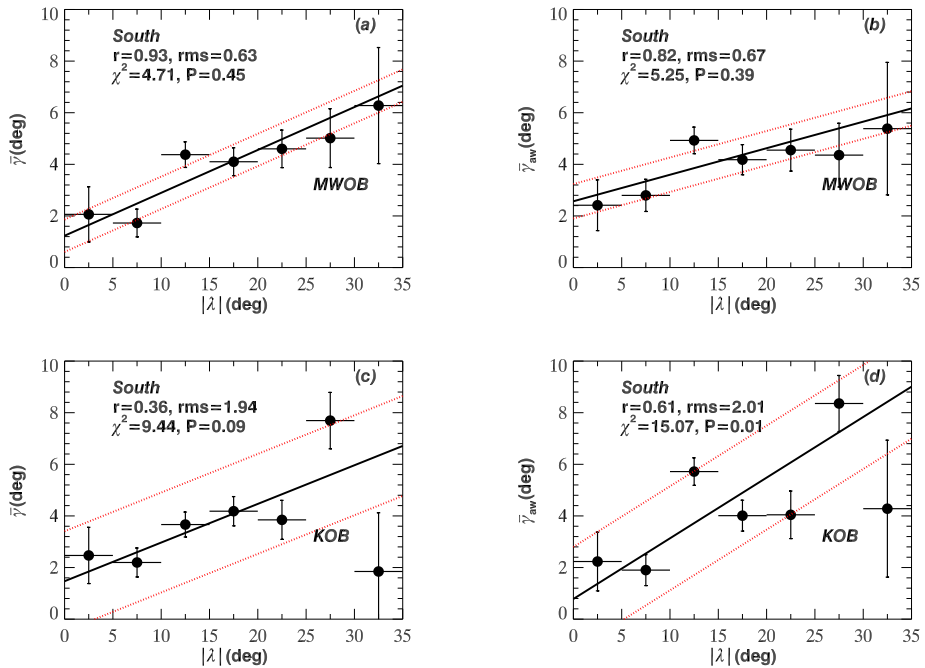


Figure 3 Mean tilt angle $[\bar{\gamma}]$ and mean area-weighted tilt angle $[\bar{\gamma}_{aw}]$ versus middle value of the corresponding 5° latitude bin, determined from Mt. Wilson Observatory (MWOB) and Kodaikanal Observatory (KOB) southern hemisphere sunspot-group data. The *continuous line* represents the corresponding linear least-square best fit and the *dotted line (red)* represents the one-rms level. The values of the correlation coefficient $[r]$, rms, and χ^2 and the corresponding probability $[P]$ are also given.

and the corresponding probability $[P]$, and the ratio m/σ_m are also given in this table. The corresponding results determined from northern and southern hemispheres’ data are given in Tables 4 and 5. The best-fit linear relations obtained from the data of some cycles are found to be reasonably good (the value of m is statistically significant, i.e. the ratio m/σ_m is ≥ 2) and the values of χ^2 are reasonably small (P is much larger than 0.05) and the fits of some other cycles are found to be not good.

Figure 4 shows cycle-to-cycle variations in different parameters: whole-sphere slope $[m_W]$, northern hemisphere slope $[m_N]$, southern hemisphere slope $[m_S]$, and north–south asymmetry in slope $[m_N - m_S]$, determined from the MWOB tilt-angle data and the area-weighted tilt-angle data. For the sake of comparison in this figure, the variation in the amplitude $[R_M]$ of the solar cycle is also shown. Note that m_W , m_N , and m_S represent the values of the slope m of whole sphere, northern hemisphere, and southern hemisphere that are given in Tables 3, 4, and 5, respectively. The uncertainty in the north–south asymmetry $m_N - m_S$ is the square root of the ratio of the sum of the squares of the standard deviations of m_N and m_S to the number of data points (number of absolute latitude bins: 7). As we can see in this figure, the patterns of m_W and m_N are similar and both seem to have no significant correlation with the amplitude of the solar cycle. It looks like there exists an anticorrelation between m_N and m_S (mainly in Figure 4a). There is a suggestion of a strong anticorrelation between m_S and the amplitude of the solar cycle, and a strong correlation between the north–south asymmetry in the slope and the amplitude of the solar cycle (mainly in Figure 4b).

Table 2 Values of the intercept [c] and the slope [m], and the corresponding standard deviations [σ_c and σ_m], respectively, of the best-fit linear relationships derived from the mean values of tilt angles and area-weighted tilt angles of sunspot groups in different 5° -latitude intervals of whole-sphere, and northern and southern hemispheres, by using the entire periods MWOB and KOB sunspot-group data. The values of correlation coefficient [r], Student's t [τ], and the corresponding probability [P], and the ratio m/σ_m are also given.

<i>Data</i>	<i>c</i>	σ_c	<i>m</i>	σ_m	<i>r</i>	τ	<i>P</i>	m/σ_m
Derived from tilt angles								
MWOB Whole	1.26	0.66	0.20	0.03	0.97	8.92	0.0001	6.67
MWOB North	1.31	0.86	0.22	0.05	0.95	6.80	0.0005	4.40
MWOB South	1.23	0.83	0.17	0.04	0.93	5.66	0.0012	4.25
KOB Whole	1.97	0.61	0.16	0.03	0.77	2.70	0.0214	5.33
KOB North	2.41	0.79	0.18	0.04	0.93	5.66	0.0012	4.50
KOB South	1.47	0.83	0.15	0.04	0.36	0.86	0.2138	3.75
Derived from area-weighted tilt angles								
MWOB Whole	2.34	0.67	0.18	0.04	0.97	8.92	0.0001	4.50
MWOB North	2.32	0.89	0.23	0.05	0.94	6.16	0.0008	4.60
MWOB South	2.57	0.90	0.10	0.05	0.82	3.20	0.0119	2.00
KOB Whole	2.39	0.81	0.20	0.04	0.79	2.88	0.0173	5.00
KOB North	4.15	1.03	0.13	0.06	0.84	3.46	0.0090	2.17
KOB South	0.78	0.99	0.24	0.05	0.61	1.72	0.0729	4.80

Figure 5 shows the relationship between slope m_W (the values of m given Table 3) of Joy's law derived from the whole-sphere area-weighted tilt-angle data of a solar cycle and the amplitude [R_M] of the solar cycle. The correlations are determined with and without the data point of Solar Cycle 15 as it has a high value and is an outlier (more outside the one-rms level, see Figure 5a). As can be seen in this figure there exists a small and insignificant anticorrelation, and the corresponding best-fit linear relations are not good. That is, the slopes of the best-fit linear equations are found to be only 1–1.4 times the corresponding standard deviations, although the values of χ^2 are smaller than that of the 5% significance level. In the case of tilt-angle data (without area weighting) the correlations are found to be much smaller (hence not shown). Overall, these results suggest that there exists only a weak linear relationship between m and R_M of a solar cycle in the case of the whole-sphere data. However, Jiao, Jiang, and Wang (2021) found the existence of a significant anticorrelation between the coefficient of Joy's law and the strength of the solar cycle by using the area-weighted tilt-angle data of the sunspot groups with polarity angular separation $> 2.5^\circ$.

Figure 6 shows the relationship between m_N (the values of m given in Table 4) obtained from tilt-angle data, and also that obtained from area-weighted tilt-angle data, in the northern hemisphere during a solar cycle and R_M of the solar cycle. As can be seen in this figure, there exist no significant correlations and the corresponding best-fit linear relations are not good. That is, the value of r is statistically insignificant. The rms is large, but this could be mainly due to the data point of Solar Cycle 15, which is an outlier. In the case of tilt-angle data, the χ^2 is significant on a more than 95% confidence level (probability P is smaller than 0.05). In the case of the area-weighted tilt-angle data, the value of χ^2 is reasonably small but the ratio m/σ_m is found to be significantly small. Overall, there exists no significant linear relationship between m_N and R_M of a solar cycle determined from the northern hemisphere's data. (The values of the slopes are positive, whereas the values of r are negative, see Figure 6. This discrepancy is due to the fact that in the linear least-square fit calculations uncertainties

Table 3 Whole sphere: Values of the intercept [c] and the slope [m], and the corresponding standard deviations [σ_c and σ_m], respectively, of the best-fit linear relationships derived from the mean values of tilt angles and area-weighted tilt angles of sunspot groups in different 5° -latitude intervals of the whole sphere during each solar cycle (SC). The values of correlation coefficient [r], χ^2 and the corresponding probability [P], the ratio m/σ_m , and the rms are also given. ^a indicates incomplete data.

SC	c	σ_c	m	σ_m	r	χ^2	P	m/σ_m	rms
Derived from tilt angles									
15 ^a	-3.29	2.41	0.55	0.15	0.82	5.38	0.25	3.67	2.93
16	0.69	1.84	0.25	0.10	0.87	5.89	0.32	2.50	1.63
17	2.29	1.48	0.18	0.08	0.53	4.58	0.47	2.25	1.62
18	1.79	1.32	0.18	0.07	0.21	8.94	0.11	2.57	2.90
19	0.21	1.20	0.20	0.06	0.95	3.19	0.67	3.33	0.75
20	1.50	1.38	0.18	0.07	0.81	4.00	0.55	2.57	1.21
21	1.47	1.45	0.22	0.08	0.95	1.45	0.92	2.75	0.72
Derived from area-weighted tilt angles									
15 ^a	-1.36	2.57	0.53	0.16	0.81	7.50	0.11	3.31	2.79
16	2.65	1.74	0.17	0.09	0.82	4.05	0.54	1.89	2.02
17	2.39	1.55	0.24	0.08	0.55	9.21	0.10	3.00	2.60
18	3.13	1.49	0.16	0.08	0.01	10.68	0.06	2.00	3.51
19	1.35	1.18	0.15	0.06	0.84	6.46	0.26	2.50	0.98
20	0.18	1.55	0.32	0.08	0.92	2.69	0.75	4.00	1.24
21	3.00	1.58	0.16	0.08	0.54	6.86	0.23	2.00	2.21

in abscissae and ordinates were taken into account, whereas in the calculations of r the uncertainties are not taken into account).

Figure 7 is the same as Figure 6, but determined from the southern hemisphere’s data (the values of m given in Table 5). As we can see in this figure m_S is correlated with R_M reasonably well in both the cases of the tilt-angle data and the area-weighted tilt-angle data, and we obtained the following linear relations.

In the case of tilt-angle data:

$$m_S = 0.61 \pm 0.17 - (0.002 \pm 0.00085)R_M, \text{ and} \tag{2}$$

in the case of area-weighted tilt-angle data:

$$m_S = 0.84 \pm 0.21 - (0.0035 \pm 0.001)R_M. \tag{3}$$

These best-fit linear Equations 2 and 3 are reasonably good, i.e. the slopes are about 2.3 and 3.5 times larger than the corresponding standard deviations, respectively. The P -values of the corresponding correlations are 0.004 and 0.01, i.e. the correlations are significant on more than the 95% confidence level. The corresponding χ^2 -values are reasonably small, i.e. much lower than the value (12.592) of the 5% level of significance. Moreover, only one data point is only slightly outside one-rms level. Overall, there exists a significant linear relationship between the slope [m_S] determined from the southern hemisphere’s data and R_M .

Figure 8 shows the relationship between north–south asymmetry in the slope [$m_N - m_S$] of a solar cycle and the amplitude [R_M] of the solar cycle, for both the cases of the tilt

Table 4 Northern hemisphere: Values of the intercept [c] and the slope [m], and the corresponding standard deviations [σ_c and σ_m], respectively, of the best-fit linear relationships derived mean values of tilt angles and area-weighted tilt angles of sunspot groups in different 5° -latitude intervals of the northern hemisphere during each solar cycle (SC). The values of correlation coefficient [r], χ^2 and the corresponding probability [P], the ratio m/σ_m , and the rms are also given. ^a indicates incomplete data.

SC	c	σ_c	m	σ_m	r	χ^2	P	m/σ_m	rms
Derived from tilt angles									
15 ^a	-5.70	3.45	0.79	0.21	0.91	4.64	0.33	3.76	2.98
16	1.43	2.24	0.18	0.12	0.78	3.27	0.66	1.50	2.12
17	5.00	2.05	0.05	0.11	0.03	5.60	0.35	0.45	2.05
18	3.93	1.86	0.14	0.10	0.31	6.15	0.29	1.40	3.50
19	0.19	1.47	0.27	0.08	0.96	2.09	0.84	3.38	0.88
20	1.24	1.82	0.15	0.10	-0.13	2.92	0.71	1.50	2.94
21	0.13	2.04	0.34	0.11	0.69	6.88	0.23	3.09	2.76
Derived from area weighted-tilt angles									
15 ^a	-0.86	3.09	0.49	0.19	0.82	6.52	0.16	2.58	2.72
16	2.20	2.14	0.15	0.11	0.48	6.08	0.30	1.36	3.23
17	3.68	2.31	0.25	0.12	0.14	10.20	0.07	2.08	6.92
18	4.84	1.91	0.13	0.10	0.06	9.34	0.10	1.30	4.30
19	1.24	1.37	0.25	0.07	0.94	1.87	0.87	3.57	0.88
20	0.96	1.95	0.25	0.10	0.14	2.64	0.75	2.50	4.23
21	2.57	2.19	0.25	0.12	0.20	12.60	0.03	2.08	3.68

angles and the area-weighted tilt angles (see also Figure 4). We obtained the following linear relations.

In the case of tilt angles:

$$m_N - m_S = -0.60 \pm 0.11 + (0.0031 \pm 0.0005)R_M, \text{ and} \tag{4}$$

in the case of area-weighted tilt angles:

$$m_N - m_S = -0.63 \pm 0.11 + (0.0036 \pm 0.0005)R_M. \tag{5}$$

In the case of Equation 4, the corresponding correlation is insignificant and χ^2 is very large mainly because the data point of Solar Cycle 15 is far from the one-rms level. However, the slope is 6.2 times larger than the corresponding standard deviation, suggesting the possibility of the existence of the linear relation between $m_N - m_S$ and R_M of a solar cycle. In the case of Equation 5 the correlation is highly significant (Student's t is 5.9 and the corresponding $P = 0.001$), the χ^2 is considerably smaller (the corresponding $P = 0.61$), only one data point is only slightly out of the one-rms interval, and moreover the slope is 7.2 times larger than the corresponding standard deviation. Overall, we find that there exists a good linear relationship between the north-south difference in the slope and the amplitude [R_M] of a solar cycle.

Table 5 Southern hemisphere: Values of the intercept [c] and the slope [m], and the corresponding standard deviations [σ_c and σ_m], respectively, of the best-fit linear relationships derived from the mean values of tilt angles and area-weighted tilt angles of sunspot groups in different 5° -latitude intervals of the southern hemisphere during each solar cycle (SC). The values of the correlation coefficient [r], χ^2 and the corresponding probability [P], the ratio m/σ_m , and the rms are also given. ^a indicates incomplete data.

SC	c	σ_c	m	σ_m	r	χ^2	P	m/σ_m	rms
Derived from tilt angles									
15 ^a	-0.33	3.06	0.31	0.19	0.38	3.67	0.45	1.63	2.88
16	0.09	2.70	0.31	0.14	0.43	8.00	0.16	2.21	4.57
17	-0.18	2.00	0.30	0.10	0.57	4.77	0.44	3.00	2.61
18	0.87	1.77	0.15	0.09	-0.03	10.60	0.06	1.67	3.08
19	1.62	1.51	0.02	0.08	0.54	1.80	0.88	0.25	1.10
20	1.57	2.04	0.24	0.11	0.64	6.40	0.27	2.18	2.57
21	2.25	2.04	0.15	0.11	0.65	5.72	0.33	1.36	1.97
Derived from area weighted-tilt angles									
15 ^a	0.73	3.81	0.38	0.24	0.69	4.54	0.34	1.58	2.76
16	2.36	2.67	0.25	0.14	0.34	3.84	0.57	1.79	3.59
17	1.11	1.79	0.21	0.09	0.32	4.04	0.54	2.33	2.69
18	4.18	1.87	-0.03	0.10	-0.28	11.47	0.04	-0.30	2.82
19	3.82	1.94	-0.14	0.10	-0.56	5.33	0.38	-1.40	1.39
20	-0.92	2.21	0.40	0.11	0.87	4.90	0.43	3.64	2.02
21	3.64	2.57	0.09	0.14	0.24	15.14	0.01	0.64	5.06

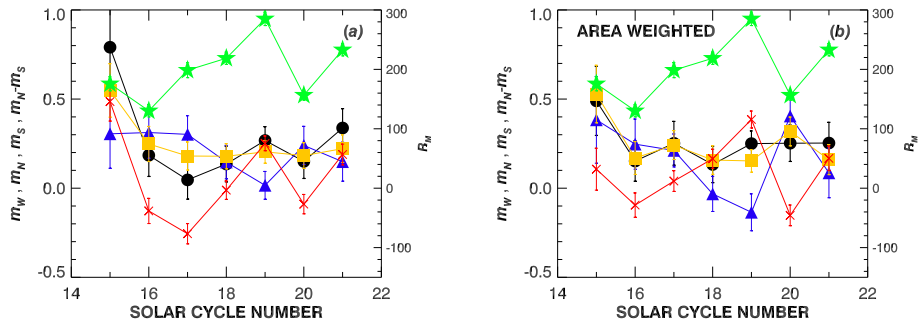


Figure 4 Cycle-to-cycle variations in different parameters: whole-sphere slope m_W (yellow filled square), northern hemisphere’s slope m_N (black filled circle), southern hemisphere’s slope m_S (blue filled triangle), and north–south asymmetry in slope $m_N - m_S$ (red cross). (a) Determined from MWOB tilt-angle data and (b) determined from MWOB area-weighted tilt-angle data. Note that the data of Solar Cycle 15 are incomplete. The variation in R_M (green filled star) is also shown.

4. Discussion and Conclusions

Study of tilt angles of solar bipolar magnetic regions is important because the tilt angles have an important role in the solar dynamo. We analyzed the data on tilt angles of sunspot groups measured at MWOB during the period 1917–1986 and at KOB during the period 1906–1986. We have used the amplitudes (the values of R_M) of Solar Cycles 15–21. We binned the daily tilt-angle data during each of the Solar Cycles 15–21 into different 5° -

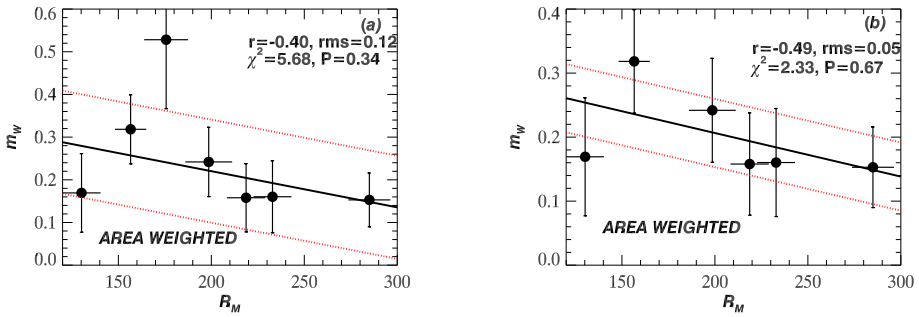


Figure 5 The slope [m_W] of Joy's law derived from the whole-sphere area-weighted tilt-angle data in 5° absolute latitude bins versus amplitude [R_M] of the solar cycle, (a) for all Cycles 15–21 and (b) for Cycles 16–21. The *continuous line* represents the corresponding linear least-square best fit and the *dotted line (red)* represents the one-rms level. The values of the correlation coefficient [r], rms, and χ^2 and the corresponding probability [P] are also given.

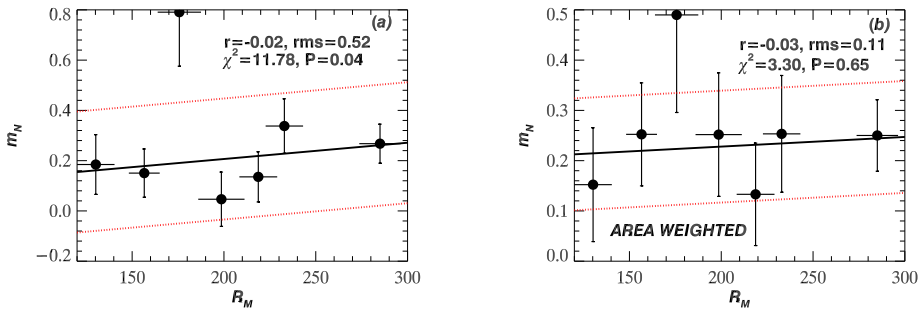


Figure 6 The slope [m_N] of Joy's law in the northern hemisphere versus amplitude [R_M] of the solar cycle derived from the average values of (a) tilt angles, and (b) area-weighted tilt angles, in 5° latitude bins. The *continuous line* represents the corresponding linear least-square best fit and the *dotted line (red)* represents the one-rms level. The values of the correlation coefficient [r], rms, and χ^2 and the corresponding probability [P] are also given.

latitude intervals and calculated the mean value of the tilt angles in each latitude interval and the corresponding standard error. We fitted these binned data to Joy's law, i.e. the linear relationship between tilt angle and latitude of an active region. The linear least-square fit calculations were carried out by taking into account the uncertainties in both the abscissa (latitude) and ordinate (mean tilt angle). The calculations were carried out by using both the tilt-angle and area-weighted tilt-angle data on the whole sphere, northern hemisphere, and southern hemisphere during the whole period and during each individual solar cycle. We find a significant difference (north–south asymmetry) between the slopes of Joy's law recovered from northern and southern hemisphere whole-period MWOB data of area-weighted tilt angles. The slope obtained from the whole-sphere MWOB data of a solar cycle is found to be weakly anti-correlated (statistically insignificant) to the amplitude [R_M] of the solar cycle. No correlation is found between the slope obtained from the northern hemisphere's data and the amplitude of the solar cycle, whereas the slope obtained from the southern hemisphere's data is found to be reasonably well anticorrelated with the amplitude of the solar cycle. In the case of area-weighted tilt-angle data, a highly statistically significant correlation is found between the north–south asymmetry in the slope of a solar cycle and

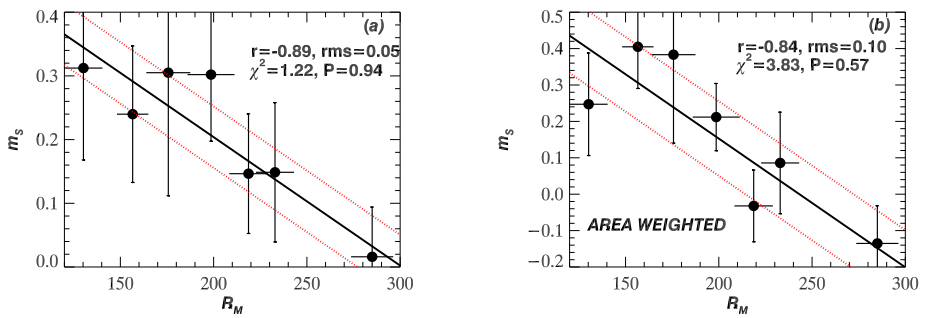


Figure 7 The slope [m_S] of Joy’s law in the southern hemisphere versus amplitude [R_M] of the solar cycle derived from the average values of (a) tilt angles and (b) area-weighted tilt angles, in 5° latitude bins. The *continuous line* represents the corresponding linear least-square best fit and the *dotted line (red)* represents the one-rms level. The values of the correlation coefficient [r], rms, and χ^2 and the corresponding probability [P] are also given.

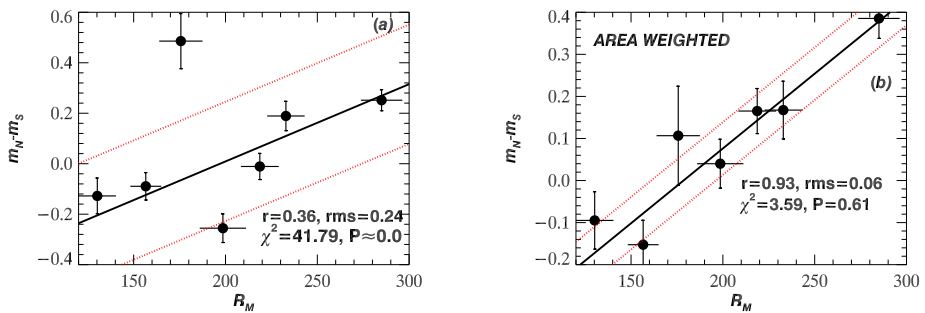


Figure 8 The hemispheric difference [$m_N - m_S$] in the slopes of Joy’s law (see also Figure 4), derived from (a) tilt angles and (b) area-weighted tilt angles shown in Figures 6 and 7, versus amplitude [R_M] of solar cycle. The *continuous line* represents the corresponding linear least-square best fit and the *dotted line (red)* represents the one-rms level. The values of the correlation coefficient [r], rms, and χ^2 and the corresponding probability [P] are also given.

the amplitude of the solar cycle. The corresponding best-fit linear equations are found to be statistically significant. These results are not found in KOB data.

McClintock and Norton (2013) analyzed the Mt. Wilson sunspot-group data (1917–1986) and found that the anticorrelation between $\langle \gamma \rangle / \langle |\lambda| \rangle$ and strength of a solar cycle is significant only in the southern hemisphere. Here, we analyzed the same data and find a significant anticorrelation between the slope and amplitude R_M of a solar cycle only from the southern hemisphere’s data. That is, the behavior of the slope in northern and southern hemispheres is closely similar to that of $\langle \gamma \rangle / \langle |\lambda| \rangle$ found by McClintock and Norton (2013). (Note that the slope m represents the latitudinal gradient of tilt angle, whereas $\langle \gamma \rangle / \langle |\lambda| \rangle$ is considered as the latitude-independent mean tilt angle.) Here, we also find the existence of a significant correlation between the north–south difference in the slope and R_M of a solar cycle. The reason why the correlation between the slope and R_M is significant only in the southern hemisphere is not clear to us. We find no significant correlation between the slope (or north–south difference $m_N - m_S$) and north–south difference in the mean area of sunspot groups (taken from Javaraiah, 2022) at the epoch of a R_M of solar cycle, indicating that no

correlation exists between the former and the north–south asymmetry in the amplitude of the solar cycle.

The m_S strongly varies and strongly anticorrelates with R_M , but m_N is almost constant (if we exclude the large value of Solar Cycle 15, see Figures 4 and 6) and there exists no correlation between m_N and R_M . Hence, there exists only a weak anti-correlation between m_W (derived from the combined northern and southern hemispheres' data) and R_M and a good positive correlation exists between $m_N - m_S$ and R_M . These results convey that it is important to determine the slope of the Joy's law separately from the tilt-angle data of the two hemispheres. However, the physical reason behind why m_S strongly anticorrelates with R_M and no correlation exists between m_N and R_M is not known to us. According to Jiao, Jiang, and Wang (2021) the Coriolis force involved in the formation of the tilt angle depends on the local expansion rate of the rising flux tube and the local rotation rate, hence the tilt angles of the two hemispheres could be independent and uncoupled. As already mentioned in Section 1, there exist north–south differences in the rotational and meridional motions of sunspot groups and also there exist cycle-to-cycle variations in these differences (e.g. Javaraiah and Ulrich, 2006). The differences in the cycle-to-cycle variations in the rotational and meridional motions of sunspot groups in northern and southern hemispheres may be responsible for the hemispheric differences in the cycle-to-cycle variations in the coefficient of Joy's law. This needs to be investigated.

Acknowledgments The author thanks the anonymous reviewer for useful comments and suggestions. The author acknowledges the work of all those who contribute to and maintain the MWOB and KOB sunspot databases. We have used the maximum values of Solar Cycles 15–21 determined by Pesnell (2018) from the time series of 13-month smoothed monthly mean values of version 2 of international sunspot number (SN) available at www.sidc.be/silso/datafiles.

Author contributions J. Javaraiah has done all the work for this manuscript.

Data Availability All data generated or analyzed during this study are included in this article.

Declarations

Competing interests The authors declare no competing interests.

References

- Bhowmik, P., Nandy, D.: 2018, Prediction of the strength and timing of sunspot cycle 25 reveal decadal-scale space environmental conditions. *Nat. Commun.* **9**, 5209. DOI. ADS.
- Carbonell, M., Oliver, R., Ballester, J.L.: 1993, On the asymmetry of solar activity. *Astron. Astrophys.* **274**, 497. ADS.
- Dasi-Espuig, M., Solanki, S.K., Krivova, N.A., Cameron, R., Peñuela, T.: 2010, Sunspot group tilt angles and the strength of the solar cycle. *Astron. Astrophys.* **518**, A7. DOI. ADS.
- D'Silva, S., Choudhuri, A.R.: 1993, A theoretical model for tilts of bipolar magnetic regions. *Astron. Astrophys.* **272**, 621. ADS.
- Fisher, G.H., Fan, Y., Howard, R.F.: 1995, Comparisons between theory and observation of active regions tilts. *Astrophys. J.* **438**, 463. DOI. ADS.
- Gigolashvili, M.S., Japaridze, D.R., Mdzinarishvili, T.G., Chargeishvili, B.B.: 2005, N-S asymmetry in the solar differential rotation during 1957–1993. *Solar Phys.* **227**, 27. DOI. ADS.
- Haber, D.A., Bradley, W., Toomre, J., Bogart, R.S., Larsen, R.M., Hill, F.: 2002, Evolving submerged meridional circulation cells within the upper convection zone revealed by ring-diagram analysis. *Astrophys. J.* **570**, 855. DOI. ADS.
- Hathaway, D.H., Wilson, R.M.: 1990, Solar rotation and the sunspot cycle. *Astrophys. J.* **357**, 271. DOI. ADS.

- Howard, R.F.: 1991, Axial tilt angles of sunspot groups. *Solar Phys.* **136**, 251. DOI. ADS.
- Javaraiah, J.: 2003, Long-term variations in the solar differential rotation. *Solar Phys.* **212**, 23. DOI. ADS.
- Javaraiah, J.: 2019, North-south asymmetry in solar activity and solar cycle prediction, IV: prediction for lengths of upcoming solar cycles. *Solar Phys.* **294**, 64. DOI. ADS.
- Javaraiah, J.: 2022, Long-term variations in solar activity: predictions for amplitude and North-south asymmetry of solar cycle 25. *Solar Phys.* **297**, 33. DOI. ADS.
- Javaraiah, J., Bertello, L., Ulrich, R.K.: 2005, An interpretation of the difference in the solar differential rotation during even and odd sunspot cycles. *Astrophys. J.* **626**, 579. DOI. ADS.
- Javaraiah, J., Gokhale, M.H.: 1997, Periodicities in the North-south asymmetry of the solar differential rotation and surface magnetic field. *Solar Phys.* **170**, 389. DOI. ADS.
- Javaraiah, J., Ulrich, R.K.: 2006, Solar-cycle-related variations in the solar differential rotation and meridional flow: a comparison. *Solar Phys.* **237**, 245. DOI. ADS.
- Jiao, Q., Jiang, J., Wang, Z.-F.: 2021, Sunspot tilt angles revisited: dependence on the solar cycle strength. *Astron. Astrophys.* **653**, A27. DOI. ADS.
- Lekshmi, B., Nandy, D., Antia, H.M.: 2018, Asymmetry in solar torsional oscillation and the sunspot cycle. *Astrophys. J.* **861**, 121. DOI. ADS.
- McClintock, B.H., Norton, A.A.: 2013, Ecovering joy’s law as a function of solar cycle, hemisphere, and longitude. *Solar Phys.* **287**, 215. DOI. ADS.
- McIntosh, S.W., Leamon, R.J., Gurman, J.B., Olive, J.-P., Cirtain, J.W., Hathaway, D.H., Burkepile, J., Milesch, M., Markel, R.S., Sitongia, L.: 2013, Hemispheric asymmetries of solar photospheric magnetism: radiative, particulate, and heliospheric impacts. *Astrophys. J.* **765**, 146. DOI. ADS.
- Muneeer, S., Sing, J.: 2002, Nature of tilt angles of sunspot groups during the 22nd solar cycle. *Solar Phys.* **209**, 321. DOI. ADS.
- Norton, A.A., Gallagher, J.C.: 2010, Solar-cycle characteristics examined in separate hemispheres: phase, gnevyshev gap, and length of minimum. *Solar Phys.* **261**, 193. DOI. ADS.
- Norton, A.A., Gilman, P.A.: 2005, Recovering solar toroidal field dynamics from sunspot location patterns. *Astrophys. J.* **630**, 1194. DOI. ADS.
- Pesnell, W.D.: 2018, Effects of version 2 of the international sunspot number on naïve predictions of solar cycle 25. *Space Weather* **16**, 1997. DOI. ADS.
- Ravindra, B., Chowdhury, P., Javaraiah, J.: 2021, Solar-cycle characteristics in kodaikanal sunspot area: North-south asymmetry, phase distribution and gnevyshev gap. *Solar Phys.* **296**, 2. DOI. ADS.
- Sivaraman, K.R., Gupta, S.S., Howard, R.F.: 1999, Measurement of Kodaikanal white-light images - IV. Axial tilt angles of sunspot groups. *Solar Phys.* **189**, 69. DOI. ADS.
- Verma, V.K.: 1993, On the North-south asymmetry of solar activity cycles. *Astrophys. J.* **403**, 797. DOI. ADS.
- Wan, M., Gao, P.-X.: 2022, Solar-cycle-related variation of differential rotation of the chromosphere. *Astrophys. J.* **939**, 111. DOI. ADS.
- Xie, J., Shi, X., Qu, Z.: 2018, North-south asymmetry of the rotation of the solar magnetic field. *Astrophys. J.* **855**, 84. DOI. ADS.
- Zharkova, V.V., Zharkov, S.I.: 2008, Tilts and polarity separation in the sunspot groups and active regions at the ascending and descending phases of the cycle 23. *Adv. Space Res.* **41**, 881. DOI. ADS.

Publisher’s Note Springer Nature remains neutral with regard to jurisdictional claims in published maps and institutional affiliations.

Springer Nature or its licensor (e.g. a society or other partner) holds exclusive rights to this article under a publishing agreement with the author(s) or other rightsholder(s); author self-archiving of the accepted manuscript version of this article is solely governed by the terms of such publishing agreement and applicable law.